



# An Improved Arrow–Hurwicz Method for the Steady-State Navier–Stokes Equations

Aziz Takhirov<sup>1</sup> · Aytekin Çıbık<sup>2</sup> · Fatma G. Eroglu<sup>3</sup> · Songül Kaya<sup>4</sup>

Received: 13 December 2022 / Revised: 20 March 2023 / Accepted: 14 June 2023 /  
Published online: 29 June 2023

© The Author(s), under exclusive licence to Springer Science+Business Media, LLC, part of Springer Nature 2023

## Abstract

This paper presents a novel Arrow–Hurwicz type method for approximating the steady-state Navier Stokes equations using the finite element method. The novel method is inspired from artificial compressibility regularization of unsteady incompressible flows and allows one to circumvent solving saddle-point equations. We derive uniform boundedness and convergence to the exact solution whenever the small data condition for uniqueness of the solution is satisfied. A two-grid version of the scheme is also discussed. Numerical schemes show that the novel scheme significantly accelerates the convergence, without any additional computational cost or decreased accuracy.

**Keywords** Arrow–Hurwicz · Steady-state Navier–Stokes equations · Two-grid

## 1 Introduction

In this paper we consider an improved Arrow–Hurwicz (AH) method for solving the steady-state Navier Stokes equations (NSE) in a domain  $\Omega \subset \mathbb{R}^d$ ,  $d \in \{2, 3\}$ , with Lipschitz boundary  $\partial\Omega$  given by

$$\mathbf{u} \cdot \nabla \mathbf{u} - \nu \Delta \mathbf{u} + \nabla p = \mathbf{f} \text{ in } \Omega, \quad (1.1)$$

---

✉ Songül Kaya  
smerdan@metu.edu.tr

Aziz Takhirov  
atakhirov@sharjah.ac.ae

Aytekin Çıbık  
abayram@gazi.edu.tr

Fatma G. Eroglu  
fguler@bartin.edu.tr

<sup>1</sup> Department of Mathematics, University of Sharjah, Sharjah, UAE

<sup>2</sup> Department of Mathematics, Gazi University, 06560 Ankara, Turkey

<sup>3</sup> Department of Mathematics, Bartın University, 74100 Bartın, Turkey

<sup>4</sup> Department of Mathematics, Middle East Technical University, 06800 Ankara, Turkey

$$\nabla \cdot \mathbf{u} = 0 \text{ in } \Omega, \tag{1.2}$$

$$\mathbf{u} = 0 \text{ on } \partial\Omega, \tag{1.3}$$

where  $\mathbf{u}$  is the fluid velocity,  $p$  the pressure,  $\nu > 0$  the kinematic viscosity and  $\mathbf{f}$  represents the prescribed external body force. A well-known result states that (1.1)–(1.3) always has a solution and its uniqueness is guaranteed under a small data condition [34]:

$$\Lambda = \nu^{-2} \mathcal{M} \|\mathbf{f}\|_{-1} \leq 1, \tag{1.4}$$

where

$$\mathcal{M} = \sup_{\mathbf{u}, \mathbf{v}, \mathbf{w} \in H_0^1(\Omega)} \frac{(\mathbf{u} \cdot \nabla \mathbf{v}, \mathbf{w})}{\|\nabla \mathbf{u}\| \|\nabla \mathbf{v}\| \|\nabla \mathbf{w}\|}. \tag{1.5}$$

The need to solve stationary NSE, (1.1)–(1.3) arises in many applications. For instance, certain hemodynamic flows occur at steady regimes [35]. More commonly, numerical benchmarking of high Reynolds number flows such the Taylor-Coutte flow [15, 29, 30] or the high Rayleigh number natural convection problems [32, 33] is performed by continuation method, where the simulations are usually initiated at smaller values of the physical parameters and are gradually increased. In such circumstances, pseudo-time stepping with unsteady flow codes usually takes a very large number of iterations or demands prohibitively fine mesh and there is a need for alternative and more efficient ways of finding the stationary solutions. One could accelerate the convergence to steady-state by adopting the pseudo-time stepping algorithm based on relaxation/penalty approach of [23], but we shall not pursue this approach here.

Numerical solution of (1.1)–(1.3) requires the linearization of the nonlinear term, commonly performed via Newton or Picard fixed point iterations [20], resulting in Oseen-type equation. The spacial discretization of (1.1)–(1.3) then requires solution of large saddle point problems [4], which are often solved by the preconditioned GMRES method [5, 31]. On the other hand, numerical schemes decoupling the equations for velocity and pressure variables are usually preferred due to their numerical efficiency. Usually such schemes are developed for unsteady flows, the most well-known of them being the projection [18] and artificial compressibility [16, 17] schemes. For steady Navier–Stokes Eqs. (1.1)–(1.3), classical methods are the Uzawa methods [4], the iterated penalty Picard method [7] and the Arrow–Hurwicz (AH) method [3].

The iterative AH scheme for solving the incompressible flow system (1.1)–(1.3) was first introduced by Temam [34]:

$$-\frac{1}{\rho} \Delta (\mathbf{u}^{n+1} - \mathbf{u}^n) + \mathbf{u}^n \cdot \nabla \mathbf{u}^{n+1} - \nu \Delta \mathbf{u}^n + \nabla p^n = \mathbf{f} \text{ in } \Omega, \tag{1.6}$$

$$\alpha (p^{n+1} - p^n) + \rho \nabla \cdot \mathbf{u}^{n+1} = 0 \text{ in } \Omega, \tag{1.7}$$

and it was shown to be weakly convergent to the unique solution  $(\mathbf{u}, p)$  of (1.1)–(1.3) under some restrictions on the value of  $\rho$  and the condition (1.4). The classical AH method is an inexact version of Uzawa algorithm and it has been applied for solving various saddle point problems, cf. [19]. The finite element analysis of the AH algorithm (1.6)–(1.7) was considered in [6], where it shown to be a contractive algorithm under certain choices of parameters. Even though the convergence rate was shown to be less than one, it was observed to require a very large number of iterations even for small Reynolds number (Re) flow problems (e.g., more than 700 iterations for  $\text{Re} = 100$  two-dimensional cavity flow). A grad-div enhanced AH algorithm (1.6)–(1.7) was recently investigated in [11]. It was shown that, under a certain choice of parameters, the additional grad-div operator improves the convergence. However,

the contractivity was shown to hold if  $\Lambda < \frac{2}{3}$ , which is more restrictive condition than (1.4). The authors also considered an AH scheme synthesized with the Anderson acceleration extrapolation technique and obtained much improved method at the cost of an additional computational complexity.

The AH Algorithm has also been studied with two-grid schemes. The general idea of two-grid methods consist of solving the computationally “cheap” iterations on a coarser mesh and then performing a few “expensive” runs on a fine mesh, thereby saving a large amount of CPU time without sacrificing the accuracy. Some notable studies in the literature are made by Ammi et al. [2], Layton et al. [26, 27], Girault et al. [13], and Li et al. [28]. For the steady state NSE, He et al. developed the two-level stabilized finite element techniques in [21] and a simplified two-level finite element method in [20]. Another related notable work is due to Du et. al. [9], where the authors extended the two-grid AH methods that were originally proposed by Xu et. al. [36, 37].

In the current study, we present novel and improved AH schemes inspired by the first order in time artificial compressibility method. When this idea is adapted to the classical AH system, the only change is observed in one term of the momentum equation. However, the acceleration on convergence speed is notable in terms of CPU time. We utilize the same idea for both single grid and two grid AH algorithms and the results obtained by various numerical examples are quite promising.

The plan of the paper is as follows: Some well-known mathematical foundations and notations used throughout the entire study are given in Sect. 2. Section 3 is devoted for introduction and mathematical analysis for improved AH scheme in single grid considerations and Sect. 4 presents similar concepts for the two grid case. Section 5 demonstrates several numerical examples which support theoretical findings and demonstrate the effectiveness of the schemes introduced. The paper is finalized with some concluding remarks.

## 2 Notations and Preliminaries

Standard notations for Sobolev spaces and corresponding norms will be used throughout the paper, see e.g., [1]. In particular,  $(\cdot, \cdot)$  and  $\| \cdot \|$  denote  $L^2(\Omega)$  inner product and the corresponding norm, respectively.  $\mathbf{H}^k$ , where  $k$  is an integer greater than zero, will denote the space of vector valued functions each of whose  $n$  components belong to  $H^k$ , the Sobolev space of real-valued functions with square integrable derivates of order up to  $k$  equipped with the usual norm  $\| \cdot \|_k$ . The dual space of  $\mathbf{H}^k$  will be denoted by  $\mathbf{H}^{-k}$ .

The equivalent weak formulation of (1.1)–(1.3) reads as follows:  $\forall (\mathbf{v}, q) \in (\mathbf{X}, Q)$ , find  $(\mathbf{u}, p) \in (\mathbf{X}, Q)$  satisfying

$$v(\nabla \mathbf{u}, \nabla \mathbf{v}) + b^*(\mathbf{u}, \mathbf{u}, \mathbf{v}) - (p, \nabla \cdot \mathbf{v}) = (\mathbf{f}, \mathbf{v}), \tag{2.1}$$

$$(\nabla \cdot \mathbf{u}, q) = 0, \tag{2.2}$$

where  $\mathbf{X} := (H_0^1(\Omega))^d$ ,  $Q := L_0^2(\Omega)$  and

$$b^*(\mathbf{u}, \mathbf{v}, \mathbf{w}) = ((\mathbf{u} \cdot \nabla) \mathbf{v}, \mathbf{w}) + \frac{1}{2} ((\nabla \cdot \mathbf{u}) \mathbf{v}, \mathbf{w}), \quad \forall \mathbf{u}, \mathbf{v}, \mathbf{w} \in X.$$

The following basic inequalities holds for all  $\mathbf{u}, \mathbf{v}, \mathbf{w} \in \mathbf{X}$ , see [14, 34]:

$$b^*(\mathbf{u}, \mathbf{v}, \mathbf{w}) \leq \mathcal{M} \|\nabla \mathbf{u}\| \|\nabla \mathbf{v}\| \|\nabla \mathbf{w}\|, \tag{2.3}$$

where  $\mathcal{M}$  is defined in (1.5).

Let  $\mathcal{T}_h$  be a conforming triangulation of the domain  $\Omega$  and let  $h = \max_{K \in \mathcal{T}_h} h_K$  denote the diameter of mesh. Then the numerical approximation of NSE reads as follows: for all  $(\mathbf{v}_h, q_h) \in (\mathbf{X}_h, Q_h)$ , find  $(\mathbf{u}_h, p_h) \in (\mathbf{X}_h, Q_h)$  satisfying

$$\nu(\nabla \mathbf{u}_h, \nabla \mathbf{v}_h) + b^*(\mathbf{u}_h, \mathbf{u}_h, \mathbf{v}_h) - (p_h, \nabla \cdot \mathbf{v}_h) = (\mathbf{f}, \mathbf{v}_h), \tag{2.4}$$

$$(\nabla \cdot \mathbf{u}_h, q_h) = 0. \tag{2.5}$$

Herein  $\mathbf{X}_h \subset \mathbf{X}$  and  $Q_h \subset Q$  are assumed to be conforming finite dimensional subspaces satisfying inf-sup condition, i.e., there is a constant  $\beta > 0$  independent of  $h$  such that

$$\inf_{q_h \in Q_h} \sup_{\mathbf{v}_h \in \mathbf{X}_h} \frac{(q_h, \nabla \cdot \mathbf{v}_h)}{\|\nabla \mathbf{v}_h\| \|q_h\|} \geq \beta > 0. \tag{2.6}$$

The error analysis in Sect. 4 uses the following estimations for trilinear term in 2d and 3d, respectively:

$$b^*(\mathbf{u}_h, \mathbf{v}_h, \mathbf{w}_h) \leq \mathcal{M} \sqrt{|\ln h|} \|\nabla \mathbf{v}_h\| \|\nabla \mathbf{w}_h\| \|\mathbf{u}_h\|, \tag{2.7}$$

$$b^*(\mathbf{u}_h, \mathbf{v}_h, \mathbf{w}_h) \leq \mathcal{M} h^{-1/2} \|\nabla \mathbf{v}_h\| \|\nabla \mathbf{w}_h\| \|\mathbf{u}_h\|, \tag{2.8}$$

we refer the reader to [14, 24] for a more detailed derivation of these results.

Similar to the continuous case, the discrete inf-sup condition (2.6) and (1.4) implies the existence and uniqueness of a solution of discrete problem (2.4)–(2.5). The stability estimate of the finite element solution is well known and the details of the proof can be found in [24, 34]: Let  $\mathbf{u}_h \in \mathbf{X}_h$ , then we get

$$\|\nabla \mathbf{u}_h\| \leq \nu^{-1} \|\mathbf{f}\|_{-1}. \tag{2.9}$$

We also recall the following finite element error estimate for the solution of (2.4)–(2.5):

**Theorem 1** *Assume  $(\mathbf{u}, p)$  be the exact solution of (2.1)–(2.2) and  $(\mathbf{u}_h, p_h)$  be the finite element solution of (2.4)–(2.5) with  $(\mathbf{X}_h, Q_h) = (P_k, P_{k-1})$ ,  $k \geq 1$  polynomials. Then we get*

$$\|\mathbf{u} - \mathbf{u}_h\| + h \left( \nu \|\nabla(\mathbf{u} - \mathbf{u}_h)\| + \|p - p_h\| \right) \leq Ch^2 \|\mathbf{f}\|. \tag{2.10}$$

### 3 Improved AH Scheme

We first describe the derivation of our novel Algorithm. To this end, consider the classical temporally first-order artificial compressibility approximation of unsteady Navier–Stokes:

$$\frac{\mathbf{u}^{n+1} - \mathbf{u}^n}{\tau} + \mathbf{u}^n \cdot \nabla \mathbf{u}^{n+1} - \nu \Delta \mathbf{u}^n + \nabla p^{n+1} = \mathbf{f} \text{ in } \Omega, \tag{3.1}$$

$$\beta(p^{n+1} - p^n) + \nabla \cdot \mathbf{u}^{n+1} = 0 \text{ in } \Omega, \tag{3.2}$$

where  $\tau \ll 1$  is a time-step and  $\beta = \mathcal{O}(1)$ . Comparing the above system to the classical AH algorithm (1.6)–(1.7), we see that  $\beta = \frac{\alpha}{\rho}$  and the main difference between the two systems is in the first term of the momentum equation. Replacing the time derivative approximation  $\frac{\mathbf{u}^{n+1} - \mathbf{u}^n}{\tau}$  by  $-\frac{1}{\rho} \Delta(\mathbf{u}^{n+1} - \mathbf{u}^n)$ , we obtain a novel AH scheme:

**Algorithm 1** (Improved AH method) Let  $\rho$  and  $\alpha$  be positive parameters.

Step 1 For all  $(\mathbf{v}_h, q_h) \in (\mathbf{X}_h, Q_h)$ , let  $(\mathbf{u}_h^0, p_h^0) \in (\mathbf{X}_h, Q_h)$  be obtained from Stokes equation satisfying

$$v(\nabla \mathbf{u}_h^0, \nabla \mathbf{v}_h) - (p_h^0, \nabla \cdot \mathbf{v}_h) = (\mathbf{f}, \mathbf{v}_h), \tag{3.3}$$

$$(q_h, \nabla \cdot \mathbf{u}_h^0) = 0. \tag{3.4}$$

Step 2 For  $n \geq 0$  and for all  $(\mathbf{v}_h, q_h) \in (\mathbf{X}_h, Q_h)$ , find  $(\mathbf{u}_h^{n+1}, p_h^{n+1}) \in (\mathbf{X}_h, Q_h)$  such that

$$\begin{aligned} \frac{1}{\rho}(\nabla(\mathbf{u}_h^{n+1} - \mathbf{u}_h^n), \nabla \mathbf{v}_h) + v(\nabla \mathbf{u}_h^{n+1}, \nabla \mathbf{v}_h) + b^*(\mathbf{u}_h^n, \mathbf{u}_h^{n+1}, \mathbf{v}_h) \\ + \frac{\rho}{\alpha}(\nabla \cdot \mathbf{u}_h^{n+1}, \nabla \cdot \mathbf{v}_h) = (p_h^n, \nabla \cdot \mathbf{v}_h) + (\mathbf{f}, \mathbf{v}_h), \end{aligned} \tag{3.5}$$

$$\alpha(p_h^{n+1} - p_h^n, q_h) + \rho(\nabla \cdot \mathbf{u}_h^{n+1}, q_h) = 0. \tag{3.6}$$

Next we discuss the uniform boundedness of the solutions to the Algorithm 1.

**Theorem 2** (Uniform boundedness) Let  $(\mathbf{u}_h, p_h) \in (\mathbf{X}_h, Q_h)$  be the solution of (2.4)–(2.5) and  $\{\mathbf{u}_h^n, p_h^n\}$  be the function sequence generated by (3.5)–(3.6). If  $\Lambda < 1$  and

$$\rho \leq \frac{2(1 - \Lambda)}{v\Lambda^2}, \tag{3.7}$$

then  $\{\mathbf{u}_h^n, p_h^n\}$  are uniformly bounded with respect to  $h$  and  $n$ .

**Proof** The first step of the proof consists of subtracting (3.5)–(3.6) from (2.4)–(2.5) to get:

$$\begin{aligned} \frac{1}{\rho}(\nabla(\mathbf{e}_h^{n+1} - \nabla \mathbf{e}_h^n, \nabla \mathbf{v}_h) + v(\nabla \mathbf{e}_h^{n+1}, \nabla \mathbf{v}_h) + b^*(\mathbf{e}_h^n, \mathbf{u}_h, \mathbf{v}_h) + b^*(\mathbf{u}_h^n, \mathbf{e}_h^{n+1}, \mathbf{v}_h) \\ + \frac{\rho}{\alpha}(\nabla \cdot \mathbf{e}_h^{n+1}, \nabla \cdot \mathbf{v}_h) - (\delta_h^n, \nabla \cdot \mathbf{v}_h) = 0, \end{aligned} \tag{3.8}$$

$$\alpha(\delta_h^{n+1} - \delta_h^n, q_h) + \rho(\nabla \cdot \mathbf{e}_h^{n+1}, q_h) = 0, \tag{3.9}$$

where  $\mathbf{e}_h^n = \mathbf{u}_h - \mathbf{u}_h^n$ ,  $\delta_h^n = p_h - p_h^n$ . Letting  $\mathbf{v}_h = \mathbf{e}_h^{n+1}$ ,  $q_h = \delta_h^n$  in (3.8)–(3.9) and using  $b^*(\mathbf{u}_h^n, \mathbf{e}_h^{n+1}, \mathbf{e}_h^{n+1}) = 0$ , we have

$$\begin{aligned} \frac{1}{2\rho} \left( \|\nabla \mathbf{e}_h^{n+1}\|^2 - \|\nabla \mathbf{e}_h^n\|^2 + \|\nabla(\mathbf{e}_h^{n+1} - \mathbf{e}_h^n)\|^2 \right) + v\|\nabla \mathbf{e}_h^{n+1}\|^2 + \frac{\rho}{\alpha} \|\nabla \cdot \mathbf{e}_h^{n+1}\|^2 \\ - (\delta_h^n, \nabla \cdot \mathbf{e}_h^{n+1}) = -b^*(\mathbf{e}_h^n, \mathbf{u}_h, \mathbf{e}_h^{n+1}) \end{aligned} \tag{3.10}$$

$$\frac{\alpha}{2\rho} (\|\delta_h^{n+1}\|^2 - \|\delta_h^n\|^2 - \|\delta_h^{n+1} - \delta_h^n\|^2) + (\nabla \cdot \mathbf{e}_h^{n+1}, \delta_h^n) = 0. \tag{3.11}$$

Also, setting  $q_h = \delta_h^{n+1} - \delta_h^n$  in (3.9) produces

$$\frac{\alpha}{\rho} \|\delta_h^{n+1} - \delta_h^n\|^2 = -(\nabla \cdot \mathbf{e}_h^{n+1}, \delta_h^{n+1} - \delta_h^n). \tag{3.12}$$

Applying Cauchy–Schwarz inequality to (3.12) yields

$$\|\delta_h^{n+1} - \delta_h^n\| \leq \frac{\rho}{\alpha} \|\nabla \cdot \mathbf{e}_h^{n+1}\|. \tag{3.13}$$

Adding (3.10) to (3.11) yields

$$\begin{aligned} & \frac{1}{2\rho} \left( \|\nabla \mathbf{e}_h^{n+1}\|^2 - \|\nabla \mathbf{e}_h^n\|^2 + \|\nabla(\mathbf{e}_h^{n+1} - \mathbf{e}_h^n)\|^2 \right) \\ & + \nu \|\nabla \mathbf{e}_h^{n+1}\|^2 + \frac{\rho}{\alpha} \left( \|\nabla \cdot \mathbf{e}_h^{n+1}\|^2 - \frac{\alpha^2}{2\rho^2} \|\delta_h^{n+1} - \delta_h^n\|^2 \right) \\ & + \frac{\alpha}{2\rho} (\|\delta_h^{n+1}\|^2 - \|\delta_h^n\|^2) \leq |b^*(\mathbf{e}_h^n, \mathbf{u}_h, \mathbf{e}_h^{n+1})|. \end{aligned} \tag{3.14}$$

On the other hand, the right hand side of the Eq. (3.14) can be bounded by (2.3), (2.9) and (1.4)

$$\begin{aligned} |b^*(\mathbf{e}_h^n, \mathbf{u}_h, \mathbf{e}_h^{n+1})| & \leq \Lambda \nu \|\nabla \mathbf{e}_h^n\| \|\nabla \mathbf{e}_h^{n+1}\| \\ & \leq \Lambda \nu (\|\nabla(\mathbf{e}_h^{n+1} - \mathbf{e}_h^n)\| + \|\nabla \mathbf{e}_h^{n+1}\|) \|\nabla \mathbf{e}_h^{n+1}\| \\ & \leq \frac{1}{2\rho} \|\nabla(\mathbf{e}_h^{n+1} - \mathbf{e}_h^n)\|^2 + \left( \Lambda \nu + \frac{\rho \Lambda^2 \nu^2}{2} \right) \|\nabla \mathbf{e}_h^{n+1}\|^2. \end{aligned} \tag{3.15}$$

Inserting the estimation (3.15) into (3.14) yields

$$\begin{aligned} & \left( \frac{1}{2\rho} + \nu - \Lambda \nu - \frac{\rho \Lambda^2 \nu^2}{2} \right) \|\nabla \mathbf{e}_h^{n+1}\|^2 + \frac{\rho}{\alpha} \left( \|\nabla \cdot \mathbf{e}_h^{n+1}\|^2 - \frac{\alpha^2}{2\rho^2} \|\delta_h^{n+1} - \delta_h^n\|^2 \right) \\ & + \frac{\alpha}{2\rho} \|\delta_h^{n+1}\|^2 \leq \frac{1}{2\rho} \|\nabla \mathbf{e}_h^n\|^2 + \frac{\alpha}{2\rho} \|\delta_h^n\|^2. \end{aligned} \tag{3.16}$$

Under the assumption (3.7), since  $\nu - \Lambda \nu - \frac{\rho \Lambda^2 \nu^2}{2} \geq 0$ , using (3.13), dropping the non-negative term in (3.16) gives

$$\frac{1}{2\rho} \|\nabla \mathbf{e}_h^{n+1}\|^2 + \frac{\alpha}{2\rho} \|\delta_h^{n+1}\|^2 \leq \frac{1}{2\rho} \|\nabla \mathbf{e}_h^n\|^2 + \frac{\alpha}{2\rho} \|\delta_h^n\|^2. \tag{3.17}$$

Therefore, one has

$$\frac{1}{2\rho} \|\nabla \mathbf{e}_h^{n+1}\|^2 + \frac{\alpha}{2\rho} \|\delta_h^{n+1}\|^2 \leq \frac{1}{2\rho} \|\nabla \mathbf{e}_h^0\|^2 + \frac{\alpha}{2\rho} \|\delta_h^0\|^2. \tag{3.18}$$

It is clear that  $\{\mathbf{u}_h^n, p_h^n\}$  is uniformly bounded if  $\mathbf{e}_h^0$  and  $\delta_h^0$  are. To show uniform boundness of  $\mathbf{e}_h^0$  and  $\delta_h^0$ , subtract (3.3)–(3.4) from (2.4)–(2.5), which results

$$\nu(\nabla \mathbf{e}_h^0, \nabla \mathbf{v}_h) - (\delta_h^0, \nabla \cdot \mathbf{v}_h) = -b(\mathbf{u}_h, \mathbf{u}_h, \mathbf{v}_h), \tag{3.19}$$

$$(q_h, \nabla \cdot \mathbf{e}_h^0) = 0. \tag{3.20}$$

Choosing  $\mathbf{v}_h = \mathbf{u}_h - \mathbf{u}_h^0 = \mathbf{e}_h^0$ ,  $q_h = p_h - p_h^0 = \delta_h^0$  in (3.19)–(3.20) and adding (3.19) to (3.20) and applying (2.3) yields

$$\nu \|\nabla \mathbf{e}_h^0\|^2 \leq \mathcal{M} \|\nabla \mathbf{u}_h\|^2 \|\nabla \mathbf{e}_h^0\|. \tag{3.21}$$

Finally, using (1.4) and (2.9) gives

$$\nu \|\nabla \mathbf{e}_h^0\| \leq \mathcal{M} \|\nabla \mathbf{u}_h\|^2 \leq \Lambda \|f\|_{-1}. \tag{3.22}$$

By inf-sup condition, it follows that

$$\|\delta_h^0\| \leq 2\Lambda \beta^{-1} \|f\|_{-1}. \tag{3.23}$$

Hence (3.18) becomes

$$\|\nabla \mathbf{e}_h^{n+1}\|^2 + \alpha \|\delta_h^{n+1}\|^2 \leq (\nu^{-2} + 4\alpha\beta^{-2})\Lambda^2 \|f\|_{-1}^2. \tag{3.24}$$

proving that  $\{\mathbf{u}_h^n, p_h^n\}$  are uniformly bounded, independent of  $n$  and  $h$ . □

**Remark 1** Note that the presence of the  $\frac{1}{\rho}(\nabla(\mathbf{u}_h^{n+1} - \mathbf{u}_h^n), \nabla \mathbf{v}_h)$  term in (3.5) is crucial in being able to control the term  $\frac{1}{2\rho} \|\nabla(\mathbf{e}_h^{n+1} - \mathbf{e}_h^n)\|^2$  in (3.15). This would not be possible with the artificial compressibility scheme (3.1).

**Remark 2** Note that since we are proving standard uniform boundedness and convergence results, the theoretical analysis is also a standard one. But the results are much improved from those in [6] in a sense that, we have no additional restriction on  $\Lambda$  besides  $\Lambda < 1$ . In addition, improved AH scheme requires much simpler inequality for  $\rho$  compared with  $\rho$  of [6].

Next, we establish the contraction property of the Algorithm 1.

**Theorem 3** Let  $(\mathbf{u}_h, p_h) \in (\mathbf{X}_h, Q_h)$  be the solution of (2.4)–(2.5) and  $\{\mathbf{u}_h^n, p_h^n\}$  be the function sequence generated by (3.5)–(3.6). Under the assumption that  $\Lambda < 1$ , the error estimate satisfies

$$\tau \|\nabla \mathbf{e}_h^{n+1}\|^2 + \frac{\alpha}{2\rho} \|\delta_h^{n+1}\|^2 \leq \kappa \left( \tau \|\nabla \mathbf{e}_h^n\|^2 + \frac{\alpha}{2\rho} \|\delta_h^n\|^2 \right), \tag{3.25}$$

where  $\tau, \kappa \in (0, 1)$  are independent of  $h$  and  $n$ .

**Proof** According to the Lemma 2, there exist a real number  $C_1$  such that  $\|\nabla \mathbf{u}_h^n\| \leq C_1$ . Utilizing inf-sup condition, (2.3), (1.4), and the inequality  $\|\nabla \cdot \mathbf{e}_h^{n+1}\| \leq \|\nabla \mathbf{e}_h^{n+1}\|$  one gets

$$\begin{aligned} \beta \|\delta_h^n\| &\leq \sup_{\mathbf{v}_h \in \mathbf{V}_h} \frac{(\delta_h^n, \nabla \cdot \mathbf{v}_h)}{\|\nabla \mathbf{v}_h\|} \\ &\leq \rho^{-1} \|\nabla \mathbf{e}_h^{n+1} - \nabla \mathbf{e}_h^n\| + \nu \|\nabla \mathbf{e}_h^{n+1}\| + \mathcal{M} \|\nabla \mathbf{e}_h^n\| \|\nabla \mathbf{u}_h\| \\ &\quad + \mathcal{M} \|\nabla \mathbf{u}_h^n\| \|\nabla \mathbf{e}_h^{n+1}\| + \rho \alpha^{-1} \|\nabla \cdot \mathbf{e}_h^{n+1}\| \\ &\leq \rho^{-1} \|\nabla \mathbf{e}_h^{n+1}\| + \rho^{-1} \|\nabla \mathbf{e}_h^n\| + \nu \|\nabla \mathbf{e}_h^{n+1}\| + \nu \Lambda \|\nabla \mathbf{e}_h^n\| + \mathcal{M} C_1 \|\nabla \mathbf{e}_h^{n+1}\| \\ &\quad + \rho \alpha^{-1} \|\nabla \mathbf{e}_h^{n+1}\| \\ &= (\rho^{-1} + \nu \Lambda) \|\nabla \mathbf{e}_h^n\| + (\rho^{-1} + \nu + \mathcal{M} C_1 + \rho \alpha^{-1}) \|\nabla \mathbf{e}_h^{n+1}\|. \end{aligned} \tag{3.26}$$

Taking the square of both sides of the Eq. (3.26) and using the fact that  $(a + b)^2 \leq 2a^2 + 2b^2$  for any real numbers  $a$  and  $b$ , we have

$$\beta^2 \|\delta_h^n\|^2 \leq 2(\rho^{-1} + \nu \Lambda)^2 \|\nabla \mathbf{e}_h^n\|^2 + 2(\rho^{-1} + \nu + \mathcal{M} C_1 + \rho \alpha^{-1})^2 \|\nabla \mathbf{e}_h^{n+1}\|^2. \tag{3.27}$$

Hence,

$$\|\nabla \mathbf{e}_h^{n+1}\|^2 \geq C_2 \|\delta_h^n\|^2 - C_3 \|\nabla \mathbf{e}_h^n\|^2, \tag{3.28}$$

where  $C_2 = \frac{1}{2} \left( \frac{\beta}{\rho^{-1} + \nu + \mathcal{M} C_1 + \rho \alpha^{-1}} \right)^2$  and  $C_3 = \left( \frac{\rho^{-1} + \nu \Lambda}{\rho^{-1} + \nu + \mathcal{M} C_1 + \rho \alpha^{-1}} \right)^2 < 1$ .

Using (3.13) and dropping the second term on the left hand side of (3.16), we get

$$\left(\frac{1}{2\rho} + D\right) \|\nabla \mathbf{e}_h^{n+1}\|^2 + \frac{\alpha}{2\rho} \|\delta_h^{n+1}\|^2 \leq \frac{1}{2\rho} \|\nabla \mathbf{e}_h^n\|^2 + \frac{\alpha}{2\rho} \|\delta_h^n\|^2. \tag{3.29}$$

where  $D = \nu - \Lambda \nu - \frac{\rho \Lambda^2 \nu^2}{2}$ . Adding and subtracting the term  $\xi \|\nabla \mathbf{e}_h^{n+1}\|^2$  to (3.29) and using (3.28) gives

$$\begin{aligned} &\left(\frac{1}{2\rho} + D - \xi\right) \|\nabla \mathbf{e}_h^{n+1}\|^2 + \frac{\alpha}{2\rho} \|\delta_h^{n+1}\|^2 \\ &\leq \left(\frac{1}{2\rho} + \xi C_3\right) \|\nabla \mathbf{e}_h^n\|^2 + \left(\frac{\alpha}{2\rho} - \xi C_2\right) \|\delta_h^n\|^2, \end{aligned} \tag{3.30}$$

where  $\xi > 0$  is to be determined. Suppose  $\frac{1}{2\rho} + D - \xi > 0$  and  $\frac{\alpha}{2\rho} - \xi C_2 > 0$ , then one can calculate the parameter  $\xi > 0$  such that

$$\frac{\frac{1}{2\rho} + \xi C_3}{\frac{1}{2\rho} + D - \xi} = \frac{\frac{\alpha}{2\rho} - \xi C_2}{\frac{\alpha}{2\rho}}. \tag{3.31}$$

Reorganizing (3.31) gives

$$\xi^2 C_2 - \left(C_2 D + \frac{\alpha}{2\rho} + \frac{1}{2\rho} (C_2 + \alpha C_3)\right) \xi + \frac{\alpha}{2\rho} D = 0. \tag{3.32}$$

The discriminant of the quadratic Eq. (3.32) is

$$\begin{aligned} b^2 - 4ac &= \left(C_2 D + \frac{\alpha}{2\rho} + \frac{1}{2\rho} (C_2 + \alpha C_3)\right)^2 - \frac{2C_2 \alpha D}{\rho} \\ &> \left(C_2 D + \frac{\alpha}{2\rho}\right)^2 - \frac{2C_2 \alpha D}{\rho} \\ &= \left(C_2 D - \frac{\alpha}{2\rho}\right)^2 \geq 0. \end{aligned} \tag{3.33}$$

Under the assumption

$$\max \left\{ 2\rho C_2 D, \frac{C_2(4\rho D + 1)}{2 - C_3} \right\} < \alpha < \frac{C_2}{C_3}, \tag{3.34}$$

(3.32) has two real, distinct roots  $\xi_{1,2} = \left(S \pm \sqrt{S^2 - \frac{2C_2 \alpha D}{\rho}}\right) / 2C_2$ , where  $S = C_2 D + \frac{1}{2\rho} (\alpha + C_2 + \alpha C_3)$ . We select

$$\xi = \frac{S - \sqrt{S^2 - \frac{2C_2 \alpha D}{\rho}}}{2C_2}. \tag{3.35}$$

Inserting (3.35) into (3.30) produces

$$\tau \|\nabla \mathbf{e}_h^{n+1}\|^2 + \frac{\alpha}{2\rho} \|\delta_h^{n+1}\|^2 \leq \kappa \left( \tau \|\nabla \mathbf{e}_h^n\|^2 + \frac{\alpha}{2\rho} \|\delta_h^n\|^2 \right), \tag{3.36}$$



where  $\tau = \frac{1}{2\rho} + D - \xi$  and  $\kappa = 1 - \frac{2\rho\xi C_2}{\alpha}$ . This completes the proof.  $\square$

One can deduce an error estimate of  $\mathbf{u} - \mathbf{u}_h$  and  $p - p_h$  by applying Theorem 3 and the triangle inequality.

**Corollary 1** *Let  $(\mathbf{u}_h, p_h)$  and  $(\mathbf{u}_h^n, p_h^n)$  be the solutions of (2.4)–(2.5) and Algorithm 1, respectively. For  $\Lambda < 1$ , the error estimate satisfies the following bound*

$$\|\nabla(\mathbf{u}_h - \mathbf{u}_h^{n+1})\|^2 \leq \kappa^{n+1} (v^{-2} + 2\alpha(\rho\tau)^{-1}\beta^{-2}) \Lambda^2 \|\mathbf{f}\|_{-1}^2, \tag{3.37}$$

$$\|p_h - p_h^{n+1}\|^2 \leq \kappa^{n+1} (2\rho\tau\alpha^{-1}v^{-2} + 4\beta^{-2}) \Lambda^2 \|\mathbf{f}\|_{-1}^2, \tag{3.38}$$

where  $\tau, \kappa \in (0, 1)$  are independent of  $h$  and  $n$ .

**Proof** From Theorem 3, we get

$$\tau \|\nabla \mathbf{e}_h^{n+1}\|^2 + \frac{\alpha}{2\rho} \|\delta_h^{n+1}\|^2 \leq \kappa \left( \tau \|\nabla \mathbf{e}_h^n\|^2 + \frac{\alpha}{2\rho} \|\delta_h^n\|^2 \right), \tag{3.39}$$

where  $\mathbf{e}_h^n = \mathbf{u}_h - \mathbf{u}_h^n$ ,  $\delta_h^n = p_h - p_h^n$ . This yields

$$\tau \|\nabla \mathbf{e}_h^{n+1}\|^2 + \frac{\alpha}{2\rho} \|\delta_h^{n+1}\|^2 \leq \kappa^{n+1} \left( \tau \|\nabla \mathbf{e}_h^0\|^2 + \frac{\alpha}{2\rho} \|\delta_h^0\|^2 \right). \tag{3.40}$$

We now use (3.22) and (3.23) to get

$$\tau \|\nabla \mathbf{e}_h^{n+1}\|^2 + \frac{\alpha}{2\rho} \|\delta_h^{n+1}\|^2 \leq \kappa^{n+1} (\tau v^{-2} + 2\alpha\rho^{-1}\beta^{-2}) \Lambda^2 \|\mathbf{f}\|_{-1}^2, \tag{3.41}$$

which produces (3.37)–(3.38).  $\square$

**Theorem 4** *Assume  $(\mathbf{u}, p)$  and  $(\mathbf{u}_h^{n+1}, p_h^{n+1})$  solve (2.1)–(2.2) and Algorithm 1, respectively. Then, we have*

$$\begin{aligned} & v \|\nabla(\mathbf{u} - \mathbf{u}_h^{n+1})\| + \|p - p_h^{n+1}\| \\ & \leq Ch + \left( \frac{v}{\sqrt{\tau}} + \sqrt{2\rho\alpha^{-1}} \right) \sqrt{\kappa^{n+1} (\tau v^{-2} + 2\alpha\rho^{-1}\beta^{-2})} \Lambda \|\mathbf{f}\|_{-1}. \end{aligned} \tag{3.42}$$

**Proof** Applying triangle inequality produces

$$\begin{aligned} & v \|\nabla(\mathbf{u} - \mathbf{u}_h^{n+1})\| + \|p - p_h^{n+1}\| \\ & \leq v \|\nabla(\mathbf{u} - \mathbf{u}_h)\| + \|p - p_h\| + v \|\nabla(\mathbf{u}_h - \mathbf{u}_h^{n+1})\| + \|p_h - p_h^{n+1}\|. \end{aligned}$$

Combining Theorem 1 and Corollary 1, yields the stated result.  $\square$

### 3.1 Extension to Nonhomogeneous and Open Boundary Conditions Case

The analysis we presented in the preceding section uses homogeneous Dirichlet boundary conditions. We now briefly comment on the extension of our AH Algorithm 1 to a more general boundary conditions case:

$$\mathbf{u} \cdot \nabla \mathbf{u} - v \Delta \mathbf{u} + \nabla p = \mathbf{f} \text{ in } \Omega, \tag{3.43}$$

$$\nabla \cdot \mathbf{u} = 0 \text{ in } \Omega, \tag{3.44}$$

$$\mathbf{u} = \mathbf{g} \text{ on } \partial\Omega_D, \tag{3.45}$$

$$-v \nabla \mathbf{u} \cdot \mathbf{n} + p \mathbf{n} = 0 \text{ on } \partial\Omega_N. \tag{3.46}$$

In the above, we assume that  $\Omega$  is bounded, locally Lipschitz domain and  $\mathbf{g} \in \mathbf{H}^{1/2}(\Omega_D)$ , which is crucial for the existence of the appropriate solenoidal extension of  $\mathbf{g}$  (still denoted by  $\mathbf{g}$ ) to  $\Omega$  [10, Lemma IX.4.2]., we look for the solution as

$$\mathbf{u} = \widehat{\mathbf{u}} + \mathbf{g},$$

where  $(\widehat{\mathbf{u}}, p)$  now solve:

$$\widehat{\mathbf{u}} \cdot \nabla \widehat{\mathbf{u}} + \widehat{\mathbf{u}} \cdot \nabla \mathbf{g} + \mathbf{g} \cdot \nabla \widehat{\mathbf{u}} - \nu \Delta \widehat{\mathbf{u}} + \nabla p = \mathbf{f} + \nu \Delta \mathbf{g} - \mathbf{g} \cdot \nabla \mathbf{g} \text{ in } \Omega, \tag{3.47}$$

$$\nabla \cdot \widehat{\mathbf{u}} = 0 \text{ in } \Omega, \tag{3.48}$$

$$\widehat{\mathbf{u}} = \mathbf{0} \text{ on } \partial\Omega_D, \tag{3.49}$$

$$-\nu \nabla \widehat{\mathbf{u}} \cdot \mathbf{n} + p \mathbf{n} = \nu \nabla \mathbf{g} \cdot \mathbf{n} \text{ on } \partial\Omega_N. \tag{3.50}$$

The derivation of the weak formulation and the extension of our Algorithm 1 to the above system is immediate: After appropriate initialization, for  $n \geq 0$  and for all  $(\mathbf{v}_h, q_h) \in (\mathbf{X}_h, Q_h)$ , find  $(\widehat{\mathbf{u}}_h^{n+1}, p_h^{n+1}) \in (\mathbf{X}_h, Q_h)$  such that

$$\begin{aligned} & \frac{1}{\rho} (\nabla(\widehat{\mathbf{u}}_h^{n+1} - \widehat{\mathbf{u}}_h^n), \nabla \mathbf{v}_h) + \nu (\nabla \widehat{\mathbf{u}}_h^{n+1}, \nabla \mathbf{v}_h) + b^*(\widehat{\mathbf{u}}_h^n, \widehat{\mathbf{u}}_h^{n+1}, \mathbf{v}_h) \\ & + b^*(\mathbf{g}, \widehat{\mathbf{u}}_h^{n+1}, \mathbf{v}_h) + b^*(\widehat{\mathbf{u}}_h^{n+1}, \mathbf{g}, \mathbf{v}_h) \\ & + \frac{\rho}{\alpha} (\nabla \cdot \widehat{\mathbf{u}}_h^{n+1}, \nabla \cdot \mathbf{v}_h) = \mathbf{F}(\mathbf{v}_h) \end{aligned} \tag{3.51}$$

$$\alpha(p_h^{n+1} - p_h^n, q_h) + \rho (\nabla \cdot \widehat{\mathbf{u}}_h^{n+1}, q_h) = 0, \tag{3.52}$$

where  $\mathbf{F}(\mathbf{v}_h)$  represents all the terms on the right-hand side. Thus, using the crucial bound

$$|b^*(\mathbf{v}, \mathbf{g}, \mathbf{v})| \leq \varepsilon \|\nabla \mathbf{v}\|^2,$$

for all  $\varepsilon > 0$ , one can extend the earlier results to this case as well.

### 4 Improved Two-Grid AH Method

For two-grid algorithm, consider conforming triangulation  $\mathcal{T}_H$  of the domain  $\Omega$  such that  $\mathcal{T}_h$  is refinement of  $\mathcal{T}_H$  with  $\mathbf{X}_H \subset \mathbf{X}_h$  and  $Q_H \subset Q_h$ . Let  $(\mathbf{X}_H, Q_H)$  be inf-sup stable spaces such that (2.6) is fulfilled. Three kinds of two grid methods are introduced by in [9]. We modify Algorithm 3 of [9] to present improvement of our method for that two grid approach.

**Algorithm 2** (Improved Two-Grid AH method) Let  $\rho$  and  $\alpha$  be positive parameters satisfying (3.7) and (3.34), respectively.

*Step 1* (Initialize on coarse grid) For all  $(\mathbf{v}_H, q_H) \in (\mathbf{X}_H, Q_H)$ , let  $(\mathbf{u}_H^0, p_H^0) \in (\mathbf{X}_H, Q_H)$  be obtained from Stokes equation satisfying

$$\nu (\nabla \mathbf{u}_H^0, \nabla \mathbf{v}_H) - (p_H^0, \nabla \cdot \mathbf{v}_H) = (\mathbf{f}, \mathbf{v}_H), \tag{4.1}$$

$$(q_H, \nabla \cdot \mathbf{u}_H^0) = 0. \tag{4.2}$$

*Step 2* (Coarse grid AH) For  $n = \overline{0, m-1}$  and for all  $(\mathbf{v}_H, q_H) \in (\mathbf{X}_H, Q_H)$ , find  $(\mathbf{u}_H^{n+1}, p_H^{n+1}) \in (X_H, Q_H)$  such that

$$\frac{1}{\rho} (\nabla(\mathbf{u}_H^{n+1} - \mathbf{u}_H^n), \nabla \mathbf{v}_H) + \nu (\nabla \mathbf{u}_H^{n+1}, \nabla \mathbf{v}_H) + b^*(\mathbf{u}_H^n, \mathbf{u}_H^{n+1}, \mathbf{v}_H)$$

$$+\frac{\rho}{\alpha}(\nabla \cdot \mathbf{u}_H^{n+1}, \nabla \mathbf{v}_H) = (p_H^n, \nabla \cdot \mathbf{v}_H) + (\mathbf{f}, \mathbf{v}_H), \tag{4.3}$$

$$\alpha(p_H^{n+1} - p_H^n, q_H) + \rho(\nabla \cdot \mathbf{u}_H^{n+1}, q_H) = 0. \tag{4.4}$$

*Step 3 (Fine grid mixed problem)* For all  $(\mathbf{v}_h, q_h) \in (\mathbf{X}_h, Q_h)$ , let  $(\mathbf{u}_{mh}, p_{mh}) \in (X_h, Q_h)$  be the solution of

$$v(\nabla \mathbf{u}_{mh}, \nabla \mathbf{v}_h) - (p_{mh}, \nabla \cdot \mathbf{v}_h) + b^*(\mathbf{u}_H^m, \mathbf{u}_{mh}, \mathbf{v}_h) = (\mathbf{f}, \mathbf{v}_h), \tag{4.5}$$

$$(\nabla \cdot \mathbf{u}_{mh}, q_h) = 0. \tag{4.6}$$

The well-posedness of the two-grid Algorithm 2 is easily established.

**Theorem 5** Assume  $\mathbf{u}_{mh}$  solves Algorithm 2, then one gets

$$\|\nabla \mathbf{u}_{mh}\| \leq v^{-1} \|\mathbf{f}\|_{-1}. \tag{4.7}$$

**Proof** Letting  $\mathbf{v}_h = \mathbf{u}_{mh}$  and  $q_h = p_{mh}$  in (4.5), and using the skew symmetry property we have

$$v\|\nabla \mathbf{u}_{mh}\|^2 = (\mathbf{f}, \mathbf{u}_{mh}). \tag{4.8}$$

Applying Cauchy–Schwarz yields the stated result. □

Next we shall establish the error bounds for Algorithm 2.

**Theorem 6** Assume  $(\mathbf{u}_{mh}, p_{mh})$  solves Algorithm 2, then the following bounds hold in  $2d$  and  $3d$ , respectively:

$$\|\nabla(\mathbf{u}_h - \mathbf{u}_{mh})\| + \|p_h - p_{mh}\| \leq C\Lambda\sqrt{|\ln h|} \left( H^2 + \sqrt{\kappa^{n+1}(v^{-2} + 2\alpha(\rho\tau)^{-1}\beta^{-2})\Lambda} \|\mathbf{f}\|_{-1} \right), \tag{4.9}$$

$$\|\nabla(\mathbf{u}_h - \mathbf{u}_{mh})\| + \|p_h - p_{mh}\| \leq C\Lambda h^{-1/2} \left( H^2 + \sqrt{\kappa^{n+1}(v^{-2} + 2\alpha(\rho\tau)^{-1}\beta^{-2})\Lambda} \|\mathbf{f}\|_{-1} \right). \tag{4.10}$$

**Proof** We begin the proof by subtracting (4.5)–(4.6) from (2.4)–(2.5):

$$v(\nabla \mathbf{e}_{mh}, \nabla \mathbf{v}_h) - (\delta_h^m, \nabla \cdot \mathbf{v}_h) + b^*(\mathbf{u}_h - \mathbf{u}_H^m, \mathbf{u}_h, \mathbf{v}_h) + b^*(\mathbf{u}_H^m, \mathbf{e}_{mh}, \mathbf{v}_h) = 0, \tag{4.11}$$

$$(\nabla \cdot \mathbf{e}_{mh}, q_h) = 0. \tag{4.12}$$

where  $\mathbf{e}_{mh} = \mathbf{u}_h - \mathbf{u}_{mh}$ ,  $\delta_h^m = p_h - p_{mh}$ . Setting  $\mathbf{v}_h = \mathbf{e}_{mh}$ ,  $q_h = \delta_h^m$  in (4.11)–(4.12), using  $b^*(\mathbf{u}_H^m, \mathbf{e}_{mh}, \mathbf{e}_{mh}) = 0$ , and adding (4.11) to (4.12), we get

$$v\|\nabla \mathbf{e}_{mh}\|^2 \leq |b^*(\mathbf{u}_h - \mathbf{u}_H^m, \mathbf{u}_h, \mathbf{e}_{mh})|. \tag{4.13}$$

Utilizing (1.4), (2.7), (2.8), (2.9), and applying Corollary 1 and Theorem 1, Poincaré’s inequality, the nonlinear term in (4.13) can be bounded as

$$\begin{aligned} |b^*(\mathbf{u}_h - \mathbf{u}_H^m, \mathbf{u}_h, \mathbf{e}_{mh})| &\leq \Lambda v\sqrt{|\ln h|} \|\nabla \mathbf{e}_{mh}\| \|\mathbf{u}_h - \mathbf{u}_H^m\| \\ &\leq \Lambda v\sqrt{|\ln h|} \|\nabla \mathbf{e}_{mh}\| (\|\mathbf{u}_h - \mathbf{u}\| + \|\mathbf{u} - \mathbf{u}_H\| + \|\mathbf{u}_H - \mathbf{u}_H^m\|) \\ &\leq \Lambda v\sqrt{|\ln h|} \|\nabla \mathbf{e}_{mh}\| \left( H^2 + C_p\sqrt{\kappa^{n+1}(v^{-2} + 2\alpha(\rho\tau)^{-1}\beta^{-2})\Lambda} \|\mathbf{f}\|_{-1} \right) \end{aligned} \tag{4.14}$$

in 2d and as

$$|b^*(\mathbf{u}_h - \mathbf{u}_H^m, \mathbf{u}_h, \mathbf{e}_{mh})| \leq \Lambda v h^{-1/2} \|\nabla \mathbf{e}_{mh}\| \left( H^2 + C_p \sqrt{\kappa^{n+1}(v^{-2} + 2\alpha(\rho\tau)^{-1}\beta^{-2})} \Lambda \|\mathbf{f}\|_{-1} \right) \tag{4.15}$$

in 3d.

Inserting (4.14), (4.15) into (4.13), we have

$$\|\nabla \mathbf{e}_{mh}\| \leq C \Lambda \sqrt{|\ln h|} \left( H^2 + \sqrt{\kappa^{n+1}(v^{-2} + 2\alpha(\rho\tau)^{-1}\beta^{-2})} \Lambda \|\mathbf{f}\|_{-1} \right) \text{ in 2d,} \tag{4.16}$$

and

$$\|\nabla \mathbf{e}_{mh}\| \leq C \Lambda h^{-1/2} \left( H^2 + \sqrt{\kappa^{n+1}(v^{-2} + 2\alpha(\rho\tau)^{-1}\beta^{-2})} \Lambda \|\mathbf{f}\|_{-1} \right) \text{ in 3d.} \tag{4.17}$$

Moreover, using inf-sup condition (2.6) yields following bound for pressure error:

$$\|\delta_h^m\| \leq \beta^{-1} \sup_{\mathbf{v}_h \in X_h} \frac{(\delta_h^m, \nabla \cdot \mathbf{v}_h)}{\|\nabla \mathbf{v}_h\|}. \tag{4.18}$$

Under the assumption (1.4), utilizing (2.7), (2.9), (4.16) produces

$$\begin{aligned} \|\delta_h^m\| &\leq \beta^{-1} \left( v \|\nabla \mathbf{e}_{mh}\| + \mathcal{M} \sqrt{|\ln h|} \|\nabla \mathbf{u}_h\| \|\mathbf{u}_h - \mathbf{u}_H^m\| + \mathcal{M} \|\nabla \mathbf{u}_H^m\| \|\nabla \mathbf{e}_h^m\| \right) \\ &\leq \beta^{-1} \left( v(1 + \Lambda) \|\nabla \mathbf{e}_{mh}\| + \Lambda v \sqrt{|\ln h|} \|\mathbf{u}_h - \mathbf{u}_H^m\| \right) \\ &\leq C \Lambda \sqrt{|\ln h|} \left( H^2 + \sqrt{\kappa^{n+1}(v^{-2} + 2\alpha(\rho\tau)^{-1}\beta^{-2})} \Lambda \|\mathbf{f}\|_{-1} \right) \end{aligned} \tag{4.19}$$

in 2d. Analogous bound is easily obtained in 3d. Combining (4.16) with (4.19) yields the stated result. □

## 5 Numerical Experiments

In this part of the paper, we present some numerical tests to verify the theoretical findings and to demonstrate the effectiveness of the proposed Algorithms 1 and 2. We first perform a convergence test with a manufactured solution. Then, we carry out a detailed comparison between the Algorithm 1 and the classical AH scheme for Kovasznay flow [25] problem. Next we extensively test our schemes on a classical lid driven cavity flow problem at different Reynolds numbers. The last numerical test will be on flow around a step problem. We consider the Taylor-Hood finite element pair throughout all computations and direct solvers for all linear systems. The finite element software FreeFem++ [22] is used for implementation along entire study.

### 5.1 Convergence Test

To measure the error and define the convergence rates, we first consider a manufactured solution of (1.1)–(1.2) in the unit square as:

$$\mathbf{u} = \begin{pmatrix} 2\theta(x^2 - x)^2(y^2 - y)(2y - 1) \\ -2\theta(y^2 - y)^2(x^2 - x)(2x - 1) \end{pmatrix}, \quad p = \theta(2x - 1)(2y - 1), \tag{5.1}$$

**Table 1** Errors and rates for  $\theta = 2, \alpha = 1$  and  $\rho = 543.1$  with a single grid Algorithm 1

$h$	$\ \mathbf{e}_h\ $	Rate	$\ \nabla \mathbf{e}_h\ $	Rate	$\ \nabla \cdot \mathbf{e}_h\ $	Rate	$\ \delta_h\ $	Rate	nb of iterations
1.77e-1	1.07e-3	-	2.67e-2	-	4.56e-4	-	1.15e-2	-	13
8.84e-2	1.95e-4	2.45	9.62e-3	1.47	3.11e-4	0.55	2.74e-3	2.1	13
4.42e-2	2.61e-5	2.9	2.57e-3	1.9	1.45e-4	1.1	5.24e-4	2.38	13
2.21e-2	2.55e-6	3.36	5.2e-4	2.31	4.96e-5	1.55	7.85e-5	2.73	13
1.11e-2	1.95e-7	3.7	8.4e-5	2.62	1.42e-5	1.81	9.4e-6	3.1	13
5.5e-3	1.33e-8	3.87	1.25e-5	2.74	3.7e-6	1.94	9.67e-7	3.28	13

**Table 2** Errors and rates for  $\theta = 1, \alpha = 1$  and  $\rho = 2240.4$  with a single grid Algorithm 1

$h$	$\ \mathbf{e}_h\ $	Rate	$\ \nabla \mathbf{e}_h\ $	Rate	$\ \nabla \cdot \mathbf{e}_h\ $	Rate	$\ \delta_h\ $	Rate	nb of iterations
1.77e-1	5.95e-4	-	1.49e-2	-	6.28e-5	-	6.29e-3	-	10
8.84e-2	1.32e-4	2.17	6.63e-3	1.17	5.5e-5	0.19	1.83e-3	1.18	10
4.42e-2	2.45e-5	2.43	2.42e-3	1.45	3.81e-5	0.52	4.67e-4	1.97	11
2.21e-2	3.31e-6	2.89	6.51e-4	1.89	1.79e-5	1.1	9.14e-5	2.35	11
1.11e-2	3.26e-7	3.34	1.32e-4	2.3	6.17e-6	1.54	1.39e-5	2.72	11
5.5e-3	2.5e-8	3.7	2.12e-5	2.64	1.77e-6	1.8	1.68e-6	3.1	11

**Table 3** CPU times (in seconds) for  $\theta = 1, \alpha = 1$  and  $\rho = 2240.4$

$h$	Single-grid	Two-grid
1.77e-1	2.08911e-1	6.1074e-2
8.84e-2	8.583463	4.07308e-1
4.42e-2	1.587391e+1	9.888664
2.21e-2	4.578917e+1	2.032775e+1
1.11e-2	1.919163e+2	7.341746e+1
5.5e-3	1.037067e+3	3.184335e+2

where  $\theta$  is used to adjust the value of  $\Lambda$ . The right-hand side  $\mathbf{f}$  corresponding to (5.1) is promptly computed. We choose  $\nu = 1, \rho = \frac{2(1 - \Lambda)}{\nu \Lambda^2}$  and  $\alpha = 1$  for varying spatial mesh sizes  $h$ . The initial velocity and pressure fields are obtained from the Stokes system. The stopping criteria is taken as

$$\max \left\{ \frac{\|\mathbf{u}_h^{n+1} - \mathbf{u}_h^n\|_\infty}{\|\mathbf{u}_h^n\|_\infty}, \frac{\|P_h^{n+1} - P_h^n\|_\infty}{\|P_h^n\|_\infty} \right\} \leq 10^{-6}.$$

Corresponding errors in various norms and convergence rates for the Algorithm 1 are presented in Tables 1 and 2. As could clearly be deduced from the table, expected rates of convergence are achieved for all quantities and the number of iterations is nearly uniform.

Next we test the two-grid the Algorithm 2 and compare the results with the single grid Algorithm 1. In this part of the experiment, we only consider the case of  $\rho = 2240.4$  and always take  $H = \frac{h}{2}$ . Firstly, the CPU times comparison for various runs are listed in Table 3. As expected, the two-grid Algorithm needs considerably less execution time.

**Table 4** Comparison of velocity and pressure errors between two the Algorithms

$h$	$\ e_h\ $		$\ \nabla e_h\ $		$\ \delta_h\ $	
	Single grid	Two grid	Single grid	Two grid	Single grid	Two grid
1.77e-1	5.95e-4	3.812226e-5	1.49e-2	2.549661e-3	6.29e-3	2.69639e-4
8.84e-2	1.32e-4	4.695747e-6	6.63e-3	6.525849e-4	1.83e-3	2.400404e-5
4.42e-2	2.45e-5	5.853814e-7	2.42e-3	1.642817e-4	4.67e-4	2.104301e-6
2.21e-2	3.31e-6	7.316313e-8	6.51e-4	4.114818e-5	9.14e-5	1.975012e-7
1.11e-2	3.26e-7	9.147053e-9	1.32e-4	1.029213e-5	1.39e-5	1.935703e-8
5.5e-3	2.5e-8	1.143242e-9	2.12e-5	2.573358e-6	1.68e-6	1.735247e-9

The errors for both grids are reported in Table 4. Interestingly enough, in this particular test, not only the two grid algorithm is more faster, but it also yields more accurate solutions.

### 5.2 Kovaszny Flow

Herein we use the well-known Kovaszny flow problem [25] to test the stability and convergence of our scheme against the classical Arrow–Hurwicz scheme of [6] and the grad-div stabilized algorithm studied in [11]. The exact solution is

$$u_1 = 1 - e^{\lambda x} \cos(2\pi y), \quad u_2 = \frac{\lambda}{2\pi} e^{\lambda x} \sin(2\pi y), \quad p = -\frac{e^{2\lambda x}}{2} + p_0,$$

where

$$\lambda = \frac{1}{2\nu} - \sqrt{\frac{1}{4\nu^2} + 4\pi^2}$$

and  $p_0 \in R^1$  is chosen so that  $p$  has a mean value zero. The flow domain is taken to be  $\Omega = (-0.5, 1) \times (-0.5, 0.5)$ , triangulated with a uniform  $100 \times 80$  mesh.

Recall that our scheme is uniformly bounded and convergent under condition (3.7):

$$\rho \leq \frac{2(1 - \Lambda)}{\nu\Lambda^2} \text{ and } \forall \alpha > 0,$$

while the classical scheme [6] has more complex condition for both  $\rho$  and  $\alpha$ :

$$\begin{aligned} &\text{if } \rho \leq \frac{1}{\nu}, \text{ then } \alpha > \frac{\rho}{2\nu(1 - \Lambda)}, \\ &\text{and if } \frac{1}{\nu} < \rho < \frac{\rho}{2\nu(1 + \Lambda)}, \text{ then } \alpha > \frac{\rho^2}{2(2 - \rho\nu(1 + \Lambda))}. \end{aligned}$$

Thus, for all schemes,  $\rho$  should not be too large, and  $\alpha$  should be chosen large for the classical scheme and the grad-div stabilized scheme [11].

We tested all the schemes for  $\nu = 0.01$  and  $\nu = 0.001$  cases for range of values of  $\rho$  and  $\alpha$ . The findings are summarized in the Tables 5 and 8. For brevity, we shall refer to our results as ‘‘AH3’’, to the results of the classical scheme as ‘‘AH1’’ and to those of the [11] as ‘‘AH2’’.

As the Tables 5, 6, 7 and 8 reveal, our scheme was observed to be always stable and convergent. However, the classical scheme either experienced numerical instability or did not converge at all in any of our simulations. The grad-div stabilized scheme converged only

**Table 5** Number of iterations needed for convergence for  $\nu = 0.01$

$\rho = 10$				$\rho = 100$			
$\alpha$	AH1	AH2	AH3	$\alpha$	AH1	AH2	AH3
1	Unstable	Unstable	110	1	Unstable	Unstable	51
50	No convergence	232	273	10	Unstable	No convergence	56
100	No convergence	440	478	100	Unstable	51	97

**Table 6**  $\rho = 500$  and  $\nu = 0.01$

$\alpha$	AH1	AH2	AH3
10	Unstable	Unstable	51
100	Unstable	Unstable	59
200	Unstable	Unstable	68
500	Unstable	Unstable	98

**Table 7** Number of iterations needed for convergence for  $\nu = 0.001$

$\rho = 10$				$\rho = 100$			
$\alpha$	AH1	AH2	AH3	$\alpha$	AH1	AH2	AH3
1	No convergence	No convergence	929	1	Unstable	Unstable	104
50	No convergence	889	903	10	Unstable	419	104
100	No convergence	892	904	100	Unstable	93	110

**Table 8**  $\rho = 500$  and  $\nu = 0.001$

$\alpha$	AH1	AH2	AH3
1	Unstable	Unstable	49
50	Unstable	No convergence	55
100	Unstable	No convergence	60
200	Unstable	No convergence	71
500	Unstable	52	102

in some cases. Interestingly, optimal parameter values for the AH3 scheme is large  $\rho$  and small  $\alpha$ , while the other schemes tend to perform better for large values of both  $\alpha$  and  $\rho$ .

### 5.3 Lid Driven Cavity Flow

In this subsection we test our Algorithms on a well known lid driven cavity flow problem. The computational domain is  $\Omega = (0, 1)^2$ , where the top lid is moving in the positive  $x$  direction with a unit speed. The boundary conditions are taken to be no-slip along other the walls. In order to avoid the irregularity of the solution at the upper corners, we consider a regularized initial data at the upper boundary as was proposed in [8]:

$$\mathbf{u}(x, 1) = (u_1(x), 0)^T$$

**Table 9** Comparison of the vertical/horizontal components of the velocity along the segment  $x$  at  $Re = 1000$  with the results of [12] on single grid

Re = 1000, vertical component				Re = 1000, horizontal component			
$x$	[12]	83907 dof	148739 dof	$y$	[12]	83907 dof	148739 dof
1.0	0.0	0.0	0.0	1.0	1.0	1.0	1.0
0.9688	-0.21388	-0.22734	-0.226477	0.9766	0.65928	0.659245	0.658424
0.9609	-0.27669	-0.293028	-0.291823	0.9688	0.57492	0.575349	0.574304
0.9531	-0.33714	-0.354132	-0.35309	0.9609	0.51117	0.511289	0.510447
0.9453	-0.39188	-0.408762	-0.40785	0.9531	0.46604	0.467068	0.46623
0.9063	-0.51550	-0.524997	-0.52369	0.8516	0.33304	0.335252	0.334406
0.8594	-0.42665	-0.424343	-0.424281	0.7344	0.18719	0.188234	0.187606
0.8047	-0.31966	-0.318506	-0.318112	0.6172	0.05702	0.0571512	0.0569494
0.5000	0.02526	0.0264927	0.0263912	0.5000	-0.06080	-0.0614573	-0.061415
0.2344	0.32235	0.324452	0.323888	0.4531	-0.10648	-0.10745	-0.107319
0.2266	0.33075	0.332948	0.332362	0.2813	-0.280189	-0.279206	-0.278857
0.1563	0.37095	0.374188	0.373423	0.1719	-0.38289	-0.386396	-0.385818
0.0938	0.32627	0.329508	0.328721	0.1016	-0.29730	-0.298378	-0.297642
0.0781	0.30353	0.305985	0.305649	0.0703	-0.22220	-0.221412	-0.220784
0.0703	0.29012	0.292448	0.292074	0.0625	-0.20196	-0.201144	-0.20041
0.0625	0.27485	0.27737	0.276599	0.0547	-0.18109	-0.180072	-0.179556
0.0	0.0	0.0	0.0	0.0	0.0	0.0	0.0

$$u_1(x) = \begin{cases} 1 - \frac{1}{4} \left( 1 - \cos \left( \frac{0.1 - x}{0.1} \pi \right) \right)^2 & 0 \leq x \leq 0.1, \\ 1 & 0.1 < x < 0.9, \\ 1 - \frac{1}{4} \left( 1 - \cos \left( \frac{x - 0.9}{0.1} \pi \right) \right)^2 & 0.9 \leq x \leq 1. \end{cases}$$

We run the code for four different values of Reynolds number,  $Re = 1000, 3200, 5000$  and  $10,000$ . In all runs, we set  $\rho = 100$  and  $\alpha = 1$ . Meshes with various resolutions were tested, and we only report the results done on two finest meshes  $96 \times 96$  and  $128 \times 128$ . All runs are again initiated by solving a steady Stokes equation. For a quantitative comparison, we use the reference values of the velocity components at the centerlines through the domain given in Ghia et al. [12]. In Table 9, we have the values obtained with the Algorithm 1 for  $Re = 1000$ . As it can be seen, the results are quite accurate and in both cases, our scheme converged in 145 iterations. Next in Table 10, we report the results obtained on the finest mesh with the two-grid Algorithm 2 at  $Re = 10000$ . The results are again satisfactory even though the flow is not fully resolved.

The streamlines patterns obtain via our methods are shown in Figs. 1 and 2. All plots demonstrate the correct formation of eddies in the corners. Finally, the iteration count vs. error plots for  $Re = 5000$  and  $10000$  are included in Fig. 3 which show overall smooth convergence to a steady state solution.

It should be pointed out that the classical AH algorithm requires over 700 iterations even  $Re = 100$  case [6] and no convergence was obtained for the  $Re = 1000$  flow for  $\alpha = Re$  and  $\rho = 1, 10, 20, 50$ . Moreover, the grad-div stabilized Arrow-Hurzwich algorithm described in [11] could not achieve the convergence in any case with the Taylor-Hood finite element pair.



**Table 10** Comparison of the vertical/horizontal components of the velocity along the segment  $x$  at  $Re = 10000$  with the results of [12] with two-grid scheme

Re = 10000, vertical component			Re = 10000, horizontal component		
$x$	[12]	148739 dof	$y$	[12]	148739 dof
1.0	0.0	0.0	1.0	1.0	1.0
0.9688	-0.54302	-0.554456	0.9766	0.47221	0.464771
0.9609	-0.52987	-0.511624	0.9688	0.47783	0.468555
0.9531	-0.49099	-0.467844	0.9609	0.48070	0.46848
0.9453	-0.45863	-0.442968	0.9531	0.47804	0.462731
0.9063	-0.41496	-0.401293	0.8516	0.34635	0.326376
0.8594	-0.36737	-0.347906	0.7344	0.20673	0.194951
0.8047	-0.30719	-0.287881	0.6172	0.08344	0.0806239
0.5000	0.00831	0.0100617	0.5000	0.03111	-0.0252313
0.2344	0.27224	0.257845	0.4531	-0.07540	-0.0664965
0.2266	0.28003	0.265312	0.2813	-0.23186	-0.216163
0.1563	0.35070	0.333565	0.1719	-0.32709	-0.310728
0.0938	0.41487	0.397532	0.1016	-0.38000	-0.369965
0.0781	0.43124	0.417205	0.0703	-0.41657	-0.408504
0.0703	0.43733	0.42632	0.0625	-0.42537	-0.421861
0.0625	0.43983	0.432345	0.0547	-0.42735	-0.431023
0.0	0.0	0.0	0.0	0.0	0.0

**Fig. 1** Streamlines:  $Re = 1000$  (left) and  $Re = 3200$  (right)

## 5.4 Channel Flow Over a Full Step

As a final qualitative numerical test, we consider a two dimensional flow in a channel with an obstacle step. The computational domain is a  $30 \times 10$  rectangle with a  $1 \times 1$  obstacle positioned at 5 units in the bottom of the channel. We use the Taylor-Hood finite element pair as in other tests with a total degree of freedom of 19177 for the mesh used in Algorithm

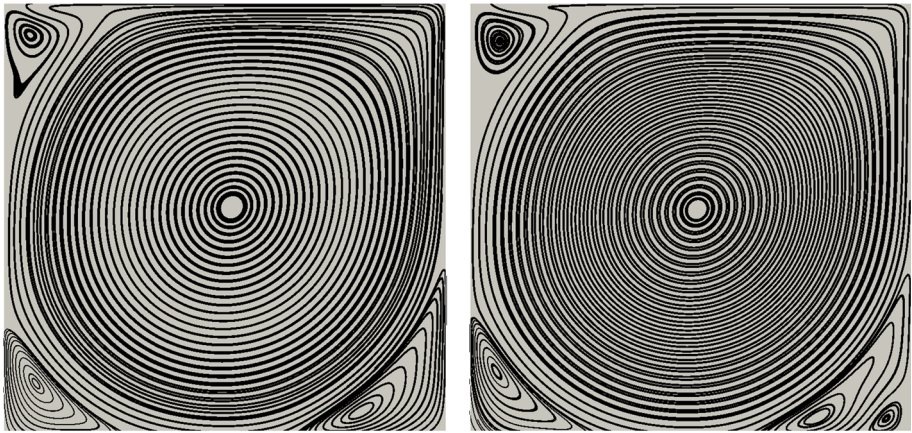


Fig. 2 Streamlines:  $Re = 5000$  (left) and  $Re = 10000$  (right)

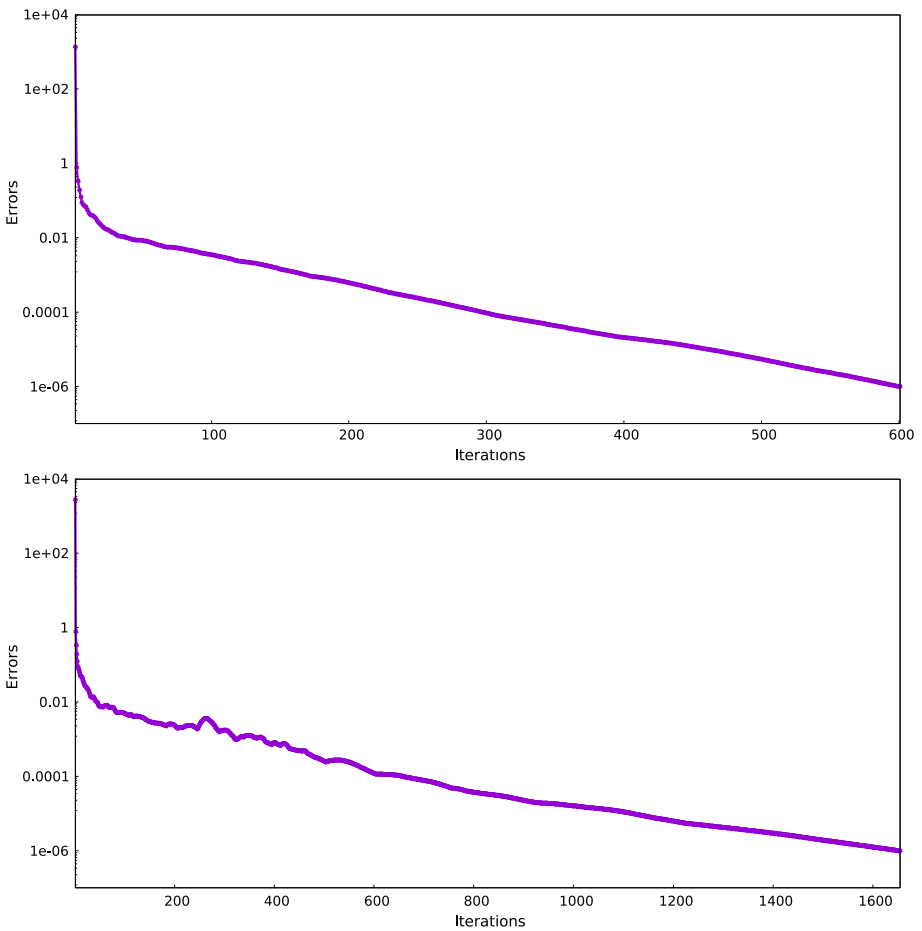
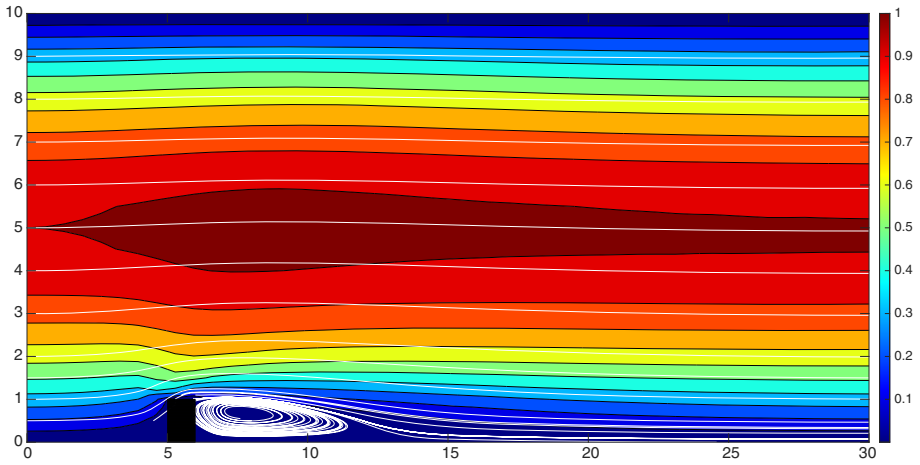
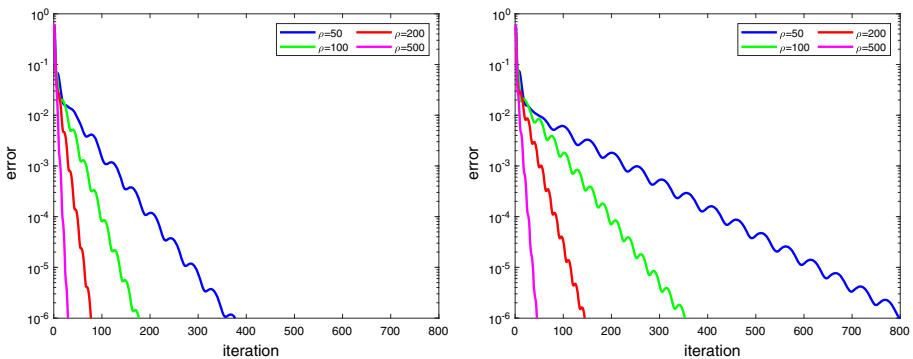


Fig. 3 Errors vs iteration count for the lid driven cavity problem:  $Re = 5000$  (top) and  $Re = 10000$  (bottom)



**Fig. 4** Streamlines over velocity contours for the channel flow with  $\nu = 0.01$



**Fig. 5** Errors vs iteration count for the channel flow: Algorithm 1 (left) and Algorithm 2 (right)

1. The coarse mesh scale is selected as  $H = \sqrt{h}$  wherever Algorithm 2 is considered. We study with  $\nu = 0.01$  along with various  $\rho$  selections and  $\alpha = \frac{1}{\nu}$ .

The streamlines over velocity contours obtained with our schemes are depicted in Fig. 4. The correct eddy formation behind the step is easily observable, which is key indicator for the accuracy of our schemes.

We also give iteration history for both schemes according to varying  $\rho$  values in Fig. 5. The pictures reveals that, as the value of  $\rho$  increases the number of iterations to reach the steady state decreases for both schemes. So the selection of  $\rho$  plays a vital role when one use these algorithms to solve any problem. On the other hand, the number of iterations to converge is higher for Algorithm 2, especially for smaller  $\rho$  values. This is due to the fact that two-grid schemes run on a coarser grid and is less resolved. However, as Table 11 reveals, although the number of iterations needed to convergence is higher for Algorithm 2, there is a meaningful difference in CPU times. Especially, for higher  $\rho$  the two-grid scheme is 3 to 5 times faster than single-grid scheme which was also observed in the preceding examples.

**Table 11** CPU times (in seconds) for varying  $\rho$  values in channel flow example

$\rho$	Single-grid	Two-grid
50	167	69
100	80	311
200	34	13
500	30	5

## 6 Concluding Remarks

In this paper a novel Arrow–Hurwicz type method for solving the steady-state Navier–Stokes equations is proposed. Key of the idea is based on changing one term in momentum equation, that is inspired from artificial compressibility method. Uniform boundedness and convergence to the exact solution under reasonable assumptions were studied. We also presented its extension to a two-grid setting and proved the corresponding convergence result as well. A comprehensive numerical studies showed a significant efficiency in terms of computing times, accuracy and robustness over the existing methods for our proposed AH algorithms.

**Author Contributions** All authors contributed equally to all parts of the study. All authors read and approved the final manuscript.

**Funding** The first author would like acknowledge the support by a University of Sharjah Grant No. 22021440125.

**Data Availability** This study has no associated data to be shared.

## Declarations

**Conflict of interest** The authors declare that they have no conflict of interest.

## References

- Adams, R.: Sobolev spaces. Academic Press, New York (1975)
- Ammi, A., Marion, M.: Nonlinear Galerkin methods and mixed finite elements: two-grid algorithms for the Navier-Stokes equations. *Numer. Math.* **68**, 189–213 (1994)
- Arrow, K.J., Hurwicz, L.: Gradient method for concave programming I: Local results. In K. J. Arrow, L. Hurwicz and H. Uzawa, (Eds.), *Studies in Linear and Nonlinear Programming*, pp 117–126, (1958)
- Benzi, M., Golub, G., Liesen, J.: Numerical solution of saddle point problems. *Acta Numer.* **14**, 1–137 (2005)
- Cao, Y., Dong, J.-L., Wang, Y.-M.: A relaxed deteriorated PSS preconditioner for nonsymmetric saddle point problems from the steady Navier-Stokes equation. *J. Comput. Appl. Math.* **273**, 41–60 (2015)
- Chen, P., Huang, J., Sheng, H.: Solving steady incompressible Navier-Stokes equations by the Arrow-Hurwicz method. *J. Comput. Appl. Math.* **311**, 100–114 (2017)
- Codina, R.: An iterative penalty method for the finite element solution of the stationary Navier-Stokes equations. *Comput. Methods Appl. Mech. Eng.* **110**, 237–262 (1993)
- de Frutos, J., John, V., Novo, J.: Projection methods for incompressible flow problems with WENO finite difference schemes. *J. Comput. Phys.* **309**, 368–386 (2016)
- Du, B., Huang, J., Zheng, H.: Two-grid Arrow-Hurwicz methods for the steady incompressible Navier-Stokes equations. *J. Sci. Comput.* **89**, 24 (2021)
- Galdi, G.P.: An introduction to the mathematical theory of the Navier-Stokes equations: steady-state problems. Springer Monographs in Mathematics. Springer, UK (2011)
- Geredeli, P., Reibold, L.G., Vargun, D., Zytoon, A.: Improved convergence of the Arrow-Hurwicz iteration for the Navier-Stokes equation via grad-div stabilization and Anderson acceleration. arXiv, (2022)

12. Ghia, U., Ghia, K.N., Shin, C.T.: High-Re solutions for incompressible flow using the Navier-Stokes equations and a multigrid method. *J. Comput. Phys.* **48**, 387–411 (1982)
13. Girault, V., Lions, J.-L.: Two-grid finite-element schemes for the transient Navier-Stokes problem. *ESAIM: Math. Modell. Numer. Anal.* **35**(5), 945–980 (2001)
14. Girault, V., Raviart, P.-A.: Finite element methods for Navier-Stokes equations: theory and algorithms. Springer Series in Computational Mathematics, Springer, USA (1986)
15. Guermond, J.L., Laguerre, R., Leorat, J., Nore, C.: Nonlinear magnetohydrodynamics in axisymmetric heterogeneous domains using a Fourier/finite element technique and an interior penalty method. *J. Comput. Phys.* **228**, 2739–2757 (2009)
16. Guermond, J.-L., Mineev, P.: High-order time stepping for the incompressible Navier-Stokes equations. *SIAM J. Sci. Comput.* **37**(6), A2656–A2681 (2015)
17. Guermond, J.-L., Mineev, P.: High-order time stepping for the Navier-Stokes equations with minimal computational complexity. *J. Comput. Appl. Math.* **310**, 92–103 (2017)
18. Guermond, J.-L., Mineev, P., Shen, J.: An overview of projection methods for incompressible flows. *Comput. Methods Appl. Mech. Eng.* **195**, 6011–6045 (2006)
19. He, B., Xu, S., Yuan, X.: On convergence of the Arrow-Hurwicz Method for saddle point problems. *J. Math. Imag. Vision* **64**, 662–671 (2022)
20. He, Y., Li, J.: Convergence of three iterative methods based on the finite element discretization for the stationary Navier-Stokes equations. *Comput. Methods Appl. Mech. Eng.* **198**(15), 1351–1359 (2009)
21. He, Y., Wang, A.: A simplified two-level method for the steady Navier-Stokes equations. *Comput. Methods Appl. Mech. Eng.* **197**(17), 1568–1576 (2008)
22. Hecht, F.: New development in FreeFem++. *J. Numer. Math.* **20**(3–4), 251–266 (2012)
23. Isik, O.R., Takhirov, A., Zheng, H.: Second order time relaxation model for accelerating convergence to steady-state equilibrium for Navier-Stokes equations. *Appl. Numer. Math.* **119**, 67–78 (2017)
24. John, V.: Finite element methods for incompressible flow problems. Springer International Publishing, Cham (2016)
25. Kovasznay, L.I.G.: Laminar flow behind a two-dimensional grid. *Math. Proc. Cambridge Philos. Soc.* **44**(1), 58–62 (1948)
26. Layton, W.: A two-level discretization method for the Navier-Stokes equations. *Comput. Math. Appl.* **26**(2), 33–38 (1993)
27. Layton, W., Tobiska, L.: A two-level method with backtracking for the Navier-Stokes equations. *SIAM J. Numer. Anal.* **35**(5), 2035–2054 (1998)
28. Li, K., Hou, Y.: An AIM and one-step Newton method for the Navier-Stokes equations. *Comput. Methods Appl. Mech. Eng.* **190**(46), 6141–6155 (2001)
29. Marcus, P.S., Tuckerman, L.S.: Simulation of flow between concentric rotating spheres. Part 1. Steady states. *J. Fluid Mech.* **185**, 1–30 (1987)
30. Marcus, P.S., Tuckerman, L.S.: Simulation of flow between concentric rotating spheres. Part 2. Transitions. *J. Fluid Mech.* **185**, 31–65 (1987)
31. Pan, J.-Y., Ng, M.K., Bai, Z.-Z.: New preconditioners for saddle point problems. *Appl. Math. Comput.* **172**, 762–771 (2006)
32. Scurtu, N., Futterer, B., Egbers, C.: Pulsating and traveling wave modes of natural convection in spherical shells. *Phys. Fluids* **22**(11), 114108 (2010)
33. Takhirov, A., Frolov, R., Mineev, P.: A direction splitting scheme for Navier-Stokes-Boussinesq system in spherical shell geometries. *Int. J. Numer. Meth. Fluids* **93**, 3507–3523 (2021)
34. Temam, R.: Navier-Stokes Equations: Theory and Numerical Analysis. Elsevier, North Holland (1979)
35. Viguerie, A., Veneziani, A.: Deconvolution-based stabilization of the incompressible Navier-Stokes equations. *J. Comput. Phys.* **391**, 226–242 (2019)
36. Xu, J.: A novel two-grid method for semilinear elliptic equations. *SIAM J. Sci. Comput.* **15**, 231–237 (1994)
37. Xu, J.: Two-grid discretization techniques for linear and nonlinear PDEs. *SIAM J. Numer. Anal.* **33**, 1759–1777 (1996)

**Publisher's Note** Springer Nature remains neutral with regard to jurisdictional claims in published maps and institutional affiliations.

Springer Nature or its licensor (e.g. a society or other partner) holds exclusive rights to this article under a publishing agreement with the author(s) or other rightsholder(s); author self-archiving of the accepted manuscript version of this article is solely governed by the terms of such publishing agreement and applicable law.